



Getting insight in the performance of noise interventions by mobile sound level measurements



Timothy Van Renterghem*, Pieter Thomas, Luc Dekoninck, Dick Botteldooren

Ghent University, Department of Information Technology, WAVES research group, Technologiepark 126, B 9052 Gent-Zwijnaarde, Belgium

ARTICLE INFO

Article history:

Received 1 February 2021

Received in revised form 7 May 2021

Accepted 26 August 2021

Keywords:

Environmental noise

Road traffic noise

Mobile noise measurements

Intervention study

ABSTRACT

In this intervention study, a mobile measurement procedure has been explored to get insight in the noise mitigation performance of a complex shaped berm near a highway. Focus was on reducing sound pressure levels on a cycling path. Mobile measurements, before and after the execution of the plans, using the same methodology, stress that both the exposure to environmental noise and the efficiency of mitigation measures can be strongly spatially dependent. Furthermore, practical constraints during the implementation of the noise abatement have a strong impact on the final efficiency. Maps based on mobile measurements show to be an interesting learning tool for spatial planners, pointing at the consequences of deviations from acoustically optimized plans. When the mobile measurements are able to provide a sufficient temporal and spectral detail, more advanced analyses are possible as well. In this work, as an example, the difference between the C-weighted and A-weighted total level allowed a more detailed understanding of the efficiency of the road traffic noise intervention.

© 2021 Elsevier Ltd. All rights reserved.

1. Introduction

Noise exposure is an important threat for the health and well-being of citizens. It is usually put at a second place when listing the most important environmental problems in large agglomerations nowadays [1]. To advance knowledge on noise abatement, measuring the effects of mitigations actually implemented could be especially interesting. However, intervention studies, including measurements before and after a measure or a set of measures are put in place, are rather scarce.

The classical way of measuring environmental sound is using a few fixed measurement stations, employing high quality equipment, where time series of sound pressure levels are recorded. This gives a highly detailed and accurate assessment of the exposure at a specific place. But such measurements lack data on the spatial variation in exposure and in abatement efficiency. Since noise is a highly variable local stressor, this is a major drawback, especially when the noise abatement solution is not sufficiently continuous due to practical constraints (e.g. a noise barrier of limited length). Such limitations could be quite detrimental for the final efficiency (see e.g. [2] or [3]), and their impact is often underestimated. Even for more continuous measures, there can still be strong differences

in noise reduction due to the nature of the diffraction process itself (depending on the distance or height relative to the barrier, see e.g. [4]) and due to the coupling with the ground effect (see e.g. [3,5,6]).

Mobile sound pressure level measurements are an interesting alternative. A number of reported case studies use mobile microphones for mapping the sound pressure levels in a specific zone [7–11]. Cyclists or walkers, equipped with a microphone and global positioning system (gps), pass along the same spots multiple times in order to reach converged sound level indicators. This convergence in road-traffic noise dominated environments occurs quite rapidly after spatio-temporal averaging [9,12], making such procedures viable.

Mobile measurements could be performed with either high-quality portable equipment, but also with so-called “noise nodes”. In the current study, the noise nodes reported by Van Renterghem et al. [13] were used. It was shown that with an adequate electro-acoustic design, the relatively cheap microphones developed for consumer electronics could be used for accurate environmental noise monitoring. A six-month lasting monitoring campaign outdoors (using the noise nodes in a fixed setup) showed that the deviation for A-weighted road traffic noise levels was less than 1 dB, in excess to the deviation amongst reference microphones themselves [13]. A third option is using smartphones as portable sound level meters. The latter attracts quite some attention nowadays, although adequate accuracy, in general, is not guaranteed [14–16]. Main issues when using the internal microphone of the

* Corresponding author at: Ghent University, Department of Information Technology, WAVES research group, Technologiepark 126, B 9052 Gent-Zwijnaarde, Belgium.

E-mail address: timothy.vanrenterghem@ugent.be (T. Van Renterghem).

smartphone is the focus on accurate representation of the speech sound frequency range, the high noise floor and thus limited dynamic range, and difficulties with proper calibration.

In this work, the use of mobile measurements is applied to assess the spatially dependent efficiency of a complex noise abatement infrastructure as put in place. The final implementation included deviations from the original plans due to practical restrictions. Mobile measurements were performed both in 2017, which will be considered as the reference situation here, and in 2020, after the abatement was finalized. Such an intervention study, using the same mobile methodology, allows a measured and detailed spatial efficiency assessment and is rather unique.

2. Materials and methods

2.1. Site description

The site of interest (51°12'37"N, 4°26'46"O) is a depressed highway near the city of Antwerp (Belgium), consisting of 8 lanes, bordered by a 6.3-m high embankment on which a cycling and walking path are present (see Fig. 1-4). The three far traffic lanes are shielded by a double row of 0.7-m high jersey's, forming a central reservation. The ring road under study is highly trafficked (exceeding 200 000 vehicles per 24 h over all lanes in September 2017) and sensitive to congestion. There is a high share of medium-heavy and heavy vehicles (35 %, September 2017).

The road segment of interest has a length of 560 m, bordered by two bridges crossing the highway. In the reference situation, the embankment consisted of rough grassland. Near its top, a small zone of tall but rather sparsely positioned trees were present (see Fig. 3), with a well-developed plant litter and humus layer beneath. This slope was yet able to reduce sound pressure levels quite well, as was previously analyzed in detail (see Ref. [17]). Nevertheless, exposure levels still exceeded 70 dB(A) on the cycling path bordering the highway in 2017.

The noise intervention consisted of adding a complex shaped berm along the full length of the cycling path (see Figs. 1 and 2). In order to increase connectivity, the cycling path was split in

two parts, where the new part allowed cyclers to go below Bridge 2 and to connect to the cycling path on the bridge itself by an additional loop (see Fig. 2 and Fig. 4 b). Near the crossing of the new and old part of the cycling path (see Fig. 2 and Fig. 4 a), a double berm was constructed to ensure noise reduction in both branches. Two ground profiles are depicted in Fig. 5, where a comparison is made with the original slope. To create the necessary space for the underpass below Bridge 2, a plateau was constructed on the slope towards the highway. To allow a future second underpass below Bridge 1, the necessary space was preserved while creating the berm, leading to a cutting in the berm (see Fig. 1 and Fig. 4 c).

Near the underpass, due to weight concerns, the berm was not prolonged and a gabion noise wall [18] was placed instead to shield cyclers when approaching the bridge (see Fig. 4 e). The gabion consisted of porous stones [19], was about 40–45 cm thick and did not contain a high surface density core. To prevent shifting of the ground bodies towards the ring road, a staircase berm shape (see Profile 1, Fig. 5) was constructed and grounds were strongly compacted. Part of the original trees were removed to allow access to the construction site.

2.2. Fixed measurements

A first fixed measurement position (MP1) was located directly bordering the highway. The second fixed point (MP2) was located on top of the embankment, directly near the cycling/walking path (see Fig. 1). The ½" type-1 electret microphones were positioned 1.75 m above the ground. In 2020, there was a nearly identical positioning as in 2017. Svantek 959 type-1 accredited measurement chains were used, measuring equivalent sound pressure levels in 1/3 octave bands, with a basic integration period of 200 ms. The equipment was weekly calibrated with a type-1 94-dB pistonphone.

MP1 is used to control for potential changes in the sound production between the two assessment periods (in 2017 and 2020) since such a close spacing primarily assesses the sound production by the road (i.e. the source strength). Variations due to sound propagation effects are nearly absent there. MP2, in contrast, will be used to validate the mobile measurement procedure.

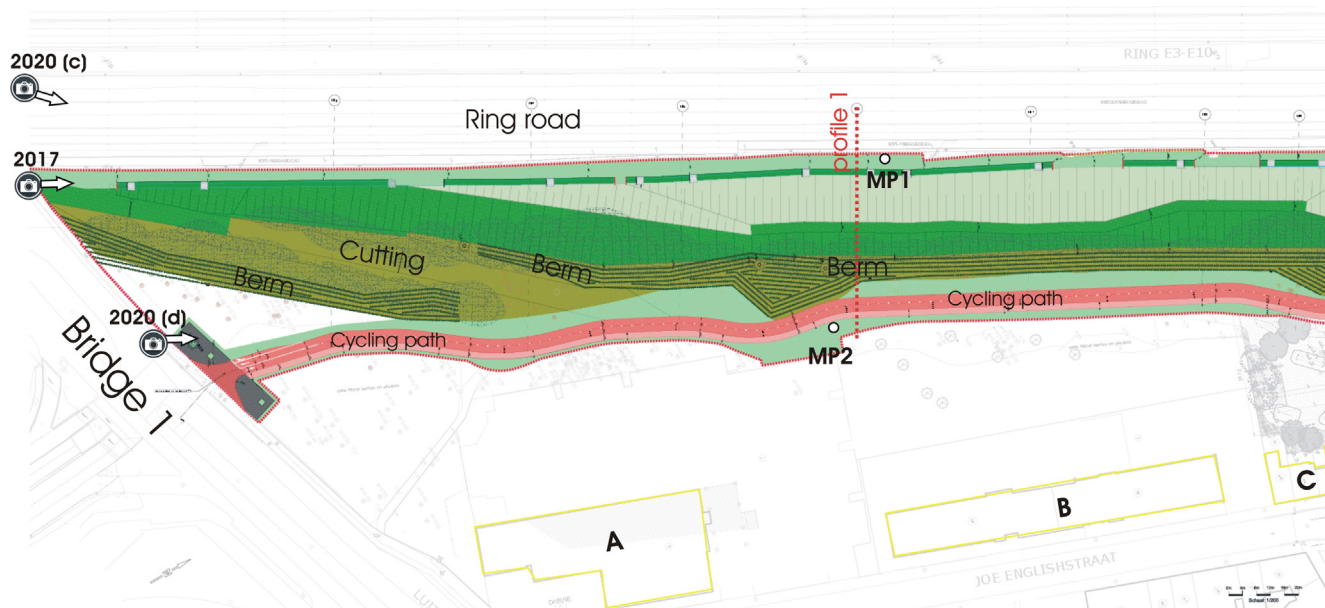


Fig. 1. Plan view of the site under study (left part) after the intervention, with indication of the key features, the location of ground profile 1 (see Fig. 5), the fixed measurement positions MP1 and MP2, and the locations where the photographs presented in Figs. 3 and 4 were taken.

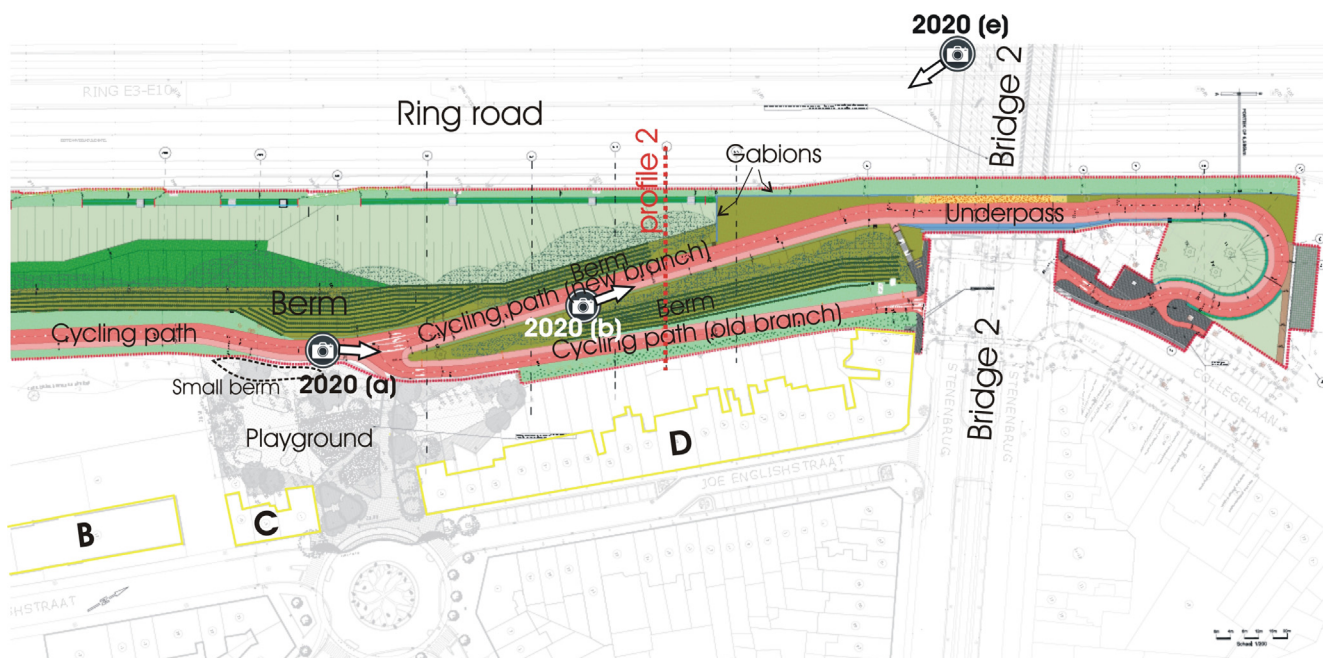


Fig. 2. Plan view of the site under study (right part) after the intervention, with indication of the key features, the location of the ground profile 2 (see Fig. 5), and the locations where the photographs presented in Fig. 4 were taken.



Fig. 3. Photograph before the intervention (2017), showing the gradually sloping grass-covered talud bordering the highway and the tree zone near its top.

Measurements in 2017 and 2020 were performed continuously during almost a full month, each time in the period September-October (from 04/09 till 02/10 in 2017; from 21/09 till 21/10 in 2020). The measurement periods at the fixed stations included each time the days on which the mobile measurements took place.

2.3. Mobile measurements

The noise nodes developed and validated in a previous study were used [13]. The operators carried a backpack, where the microphone and gps module stuck out. Multiple operators (maximum 3 simultaneously) repeatedly walked along a number of predefined paths in the zone under study. The operators were instructed to walk slowly and to reduce the self-made noise (e.g. own footsteps). Measurements were performed between morning and evening rush hours. In 2017, these measurements were distributed over 4 different days (04/09, 05/09, 07/09, 08/09), for a total of 40.6 h of measurements. In 2020, distributed over 2 days (21/09 and 22/09), 24.3 h of measurements were collected. Calibration with a type-1 94-dB pistonphone was performed at each device at the beginning of each measurement day.

The mobile equipment basically measured 1/3 octave bands at an integration period of 1/8 s. The sound pressure level measurement and the location data were linked based on the clock readings of the single board computer steering both processes. Along the walking paths, data were aggregated at fixed intervals of 5 m, with a 50 % overlap between successive aggregation points.

In Fig. 6, the time duration of the measurements at each spatial aggregation point in 2017 and 2020 is shown. There was a strong focus on the cycling path and most measurements were made there. Occasionally, passages on the bridges and in the street behind the first line of buildings parallel to the highway were made. Streets further away were considered to a limited extent only as local road traffic is dominant there, making that the effects of the noise interventions are expected to be very limited in that zone. Nevertheless, these measurements provide a global estimate of the exposure levels, but should not be used for a detailed analysis. In Appendix A, convergence of the measurements is quantified at each spatial aggregation point.

The noise indicators analyzed here were $L_{A,50}$, L_C-L_A and the spectral “centre-of-gravity” (COG). $L_{A,50}$ is the median A-weighted total sound pressure level and a good indicator for road traffic noise in case of continuous traffic. $L_{A,50}$ showed to be a stable parameter as deduced from the mobile measurements. In case of dominant and continuous road traffic as is present along the cycling path, $L_{A,50}$ is nearly identical to the equivalent sound pressure level $L_{A,eq}$. The median values are calculated based on the 1/8 s equivalent sound pressure levels belonging to a specific aggregation point. The noise reduction efficiency of the intervention at location i can then be calculated as:

$$\Delta L_{A,50,i} = L_{A,50,i,2017} - L_{A,50,i,2020} \tag{1}$$

L_C-L_A is the C-weighted total sound pressure level minus the A-weighted total level. In theory, C-weighting is used to account for the frequency dependent sensitivity of the human hearing system at 100 dB (at a reference sound frequency of 1 kHz), while A-weighting is applicable to 40 dB (at 1 kHz). At higher sound pressure levels, the weight of low frequencies is higher than at 40 dB. A large value for L_C-L_A indicates a (relative) dominance of low



Fig. 4. Photographs after the noise interventions in 2020, taken at the 5 points as indicated in Figs. 1 and 2. In (a), the crossing between the old part of the cycling path, and the part running towards the underpass is shown. In (b), the transition between the double berm zone and the gabion walls (just in front of the bridge) is depicted. In (c), the berm can be seen from the highway, including the cutting for a future underpass. In (d), a view is provided on the slightly raised berm as seen from the cycling path. In (e), the gabion noise walls is shown as seen from Bridge 2.

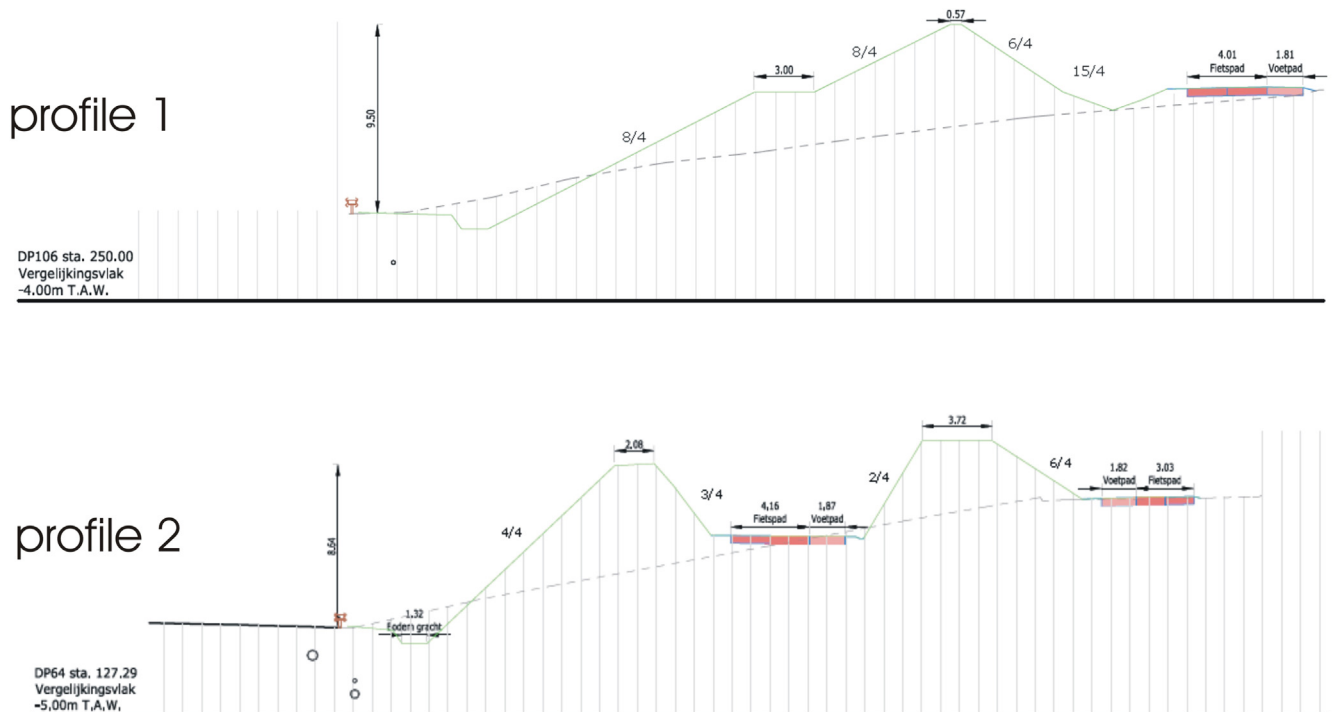


Fig. 5. Ground profiles (2020) at the two locations indicated in Figs. 1 and 2. The dashed lines show the slopes of the original taluds that were present before the intervention (2017).

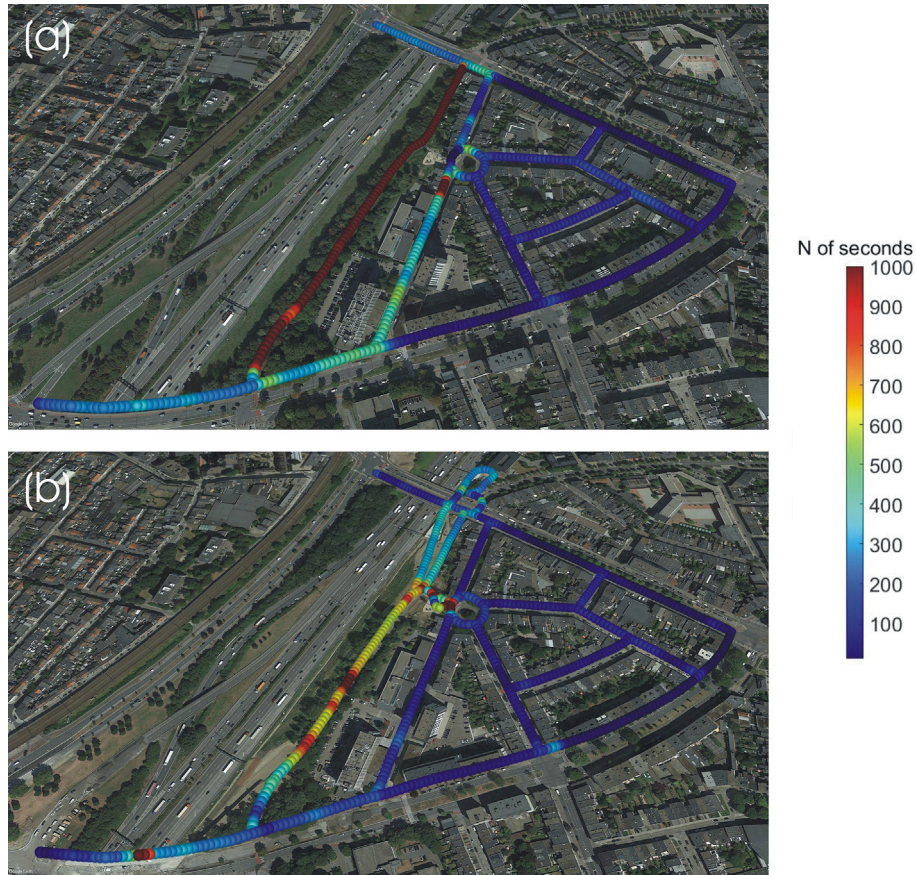


Fig. 6. Time duration of measurements (expressed in seconds) at each spatial aggregation point during the 2017 (a) and 2020 (b) mobile measurement campaigns.

sound frequencies in the spectrum. Since A-weighting and C-weighting are commonly found on (commercial) sonometers, this is an indicator that has a wide applicability. For each 1/8 s equivalent sound pressure level, the L_C-L_A indicator is first calculated, and then the median is taken over all datapoints belonging to a specific aggregation point. When comparing the 2017 and 2020 situation, the shift in L_C-L_A due to the intervention at location i is consequently calculated by:

$$\Delta(L_C - L_A)_i = L_C - \widehat{L_A} \Big|_{i,2017} - L_C - \widehat{L_A} \Big|_{i,2020} \quad (2)$$

The spectral centre-of-gravity (COG) is an indicator similar to L_C-L_A , pointing at where most acoustic energy is located in the frequency spectrum. Similarly to L_C-L_A , the COG is calculated for each 1/8 s equivalent sound pressure level spectrum, and then the median is taken over all datapoints corresponding to aggregation point i :

$$COG, i = \frac{\int_{80\text{Hz}}^{8\text{kHz}} f_c \cdot 10^{\frac{10}{10} p f_c i}}{\int_{80\text{Hz}}^{8\text{kHz}} 10^{\frac{10}{10} p f_c i}} \Big|_i \quad (3)$$

The shift in COG due to the intervention is consequently calculated as :

$$\Delta COG, i = COG_{i,2017} - COG_{i,2020} \quad (4)$$

The walked trajectory passed very closely to the fixed measurement point MP2 near the cycling path. There, operators occasionally halted to increase the number of samples to allow a good comparison with the fixed measurements.

3. Results

3.1. Validation of the mobile measurement procedure

After removal of hours with any rain or averaged hourly wind speeds exceeding 5 m/s (measured at 10 m high), the $L_{A,50}$ over the full monitoring period (roughly one month) was equal to 82.7 dB(A) in 2017, and 82.6 dB(A) in 2020, at fixed station MP1. Note that this small difference is much lower than the accuracy one gets with type-1 microphones [20]. A similar conclusion can be drawn from the mobile measurements on Bridge 1. There, both in 2017 and 2020, a sufficient number of measurements were available to allow such a comparison. The difference in exposure $\Delta L_{A,50}$ gives values equal to -1 , 0 and $+1$ dB(A). At this location, the highway noise is dominant, and there is direct line-of-sight propagation, without any interaction with the mitigation interventions. Note that at Bridge 2, a similar analysis is not possible given the limited number of measurements in the 2020 campaign (see Fig. 6 b). Both findings thus show that a direct comparison of levels is possible in both periods, without the need for correcting for (potentially) different road traffic conditions.

The difference between the fixed stations MP1 and MP2, for corresponding 5-minute $L_{A,50}$ values, characterizes the propagation of sound between the road and the cycling path. This transmission loss was assessed during the 2017 and 2020 measurement campaigns, for each 5-minute interval :

$$TL_{1-2,2017} = L_{A,50,MP1,2017} - L_{A,50,MP2,2017} \quad (5)$$

$$TL_{1-2,2020} = L_{A,50,MP1,2020} - L_{A,50,MP2,2020} \quad (6)$$

In 2017, TL_{1-2} is illustrative for the sound reduction provided by the grass-covered slope and forms the reference situation (before the intervention took place). In 2020, TL_{1-2} is further increased by the presence of the raised berm. In this way of processing, the propagation is largely separated from (momentary) source strength variations.

The difference between the transmission losses in 2017 and 2020 is an accurate assessment of the abatement efficiency ε at MP2 on the cycling path:

$$\varepsilon = TL_{1-2,2020} - TL_{1-2,2017} \tag{7}$$

The distribution of $TL_{1-2,2017}$ and $TL_{1-2,2020}$, over the full month of measurements, shows some variation (characterized by an interquartile distance of 1.3 dB(A) in 2017, and 1.9 dB(A) in 2020). This can be due to changing propagation conditions (more precisely : variations in air absorption, changing soil water content of the natural grounds forming the slope or berm, and refraction by either wind speed or temperature gradients – for more information

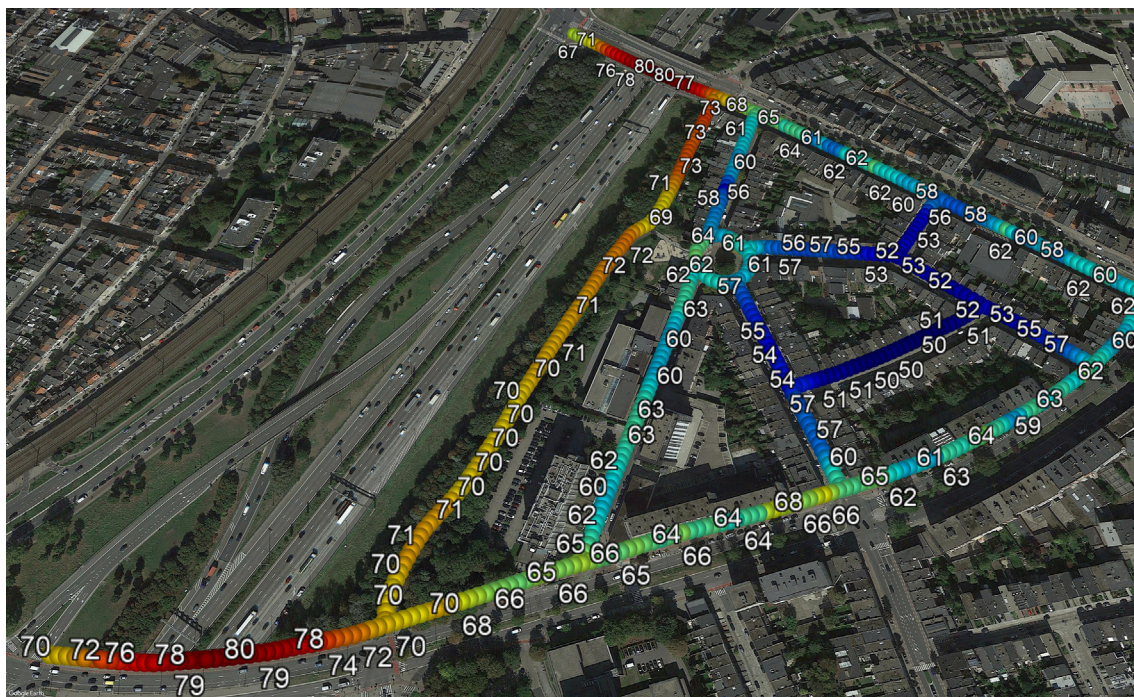


Fig. 7. $L_{A,50}$ map as measured before the intervention (2017) in dB(A).

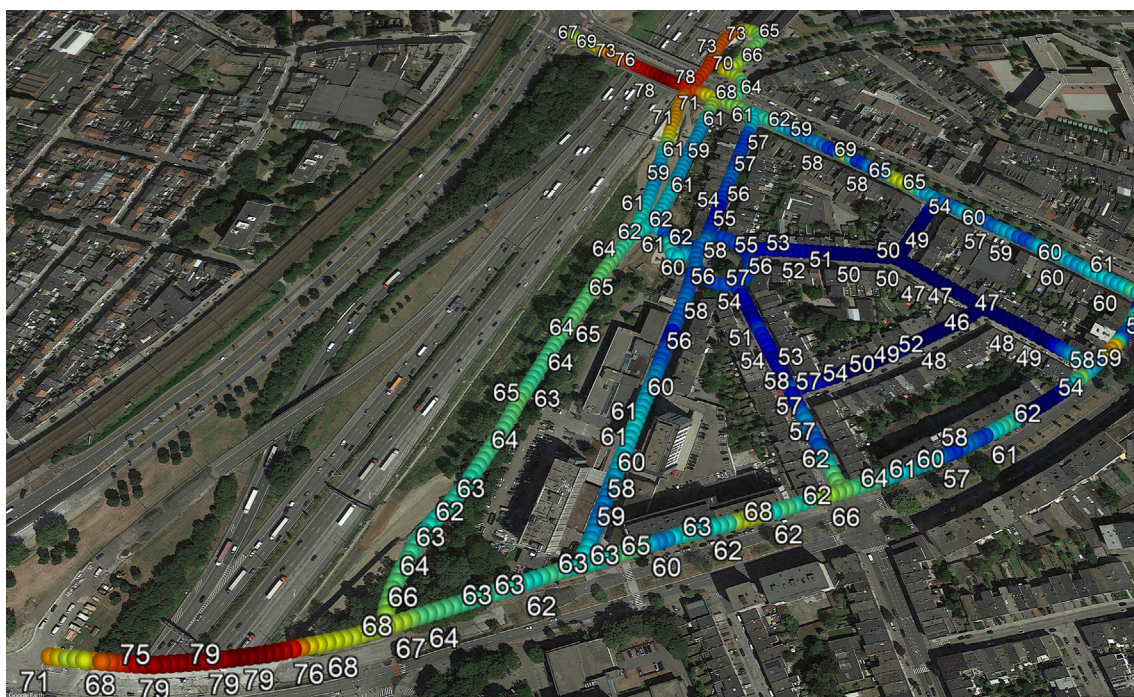


Fig. 8. $L_{A,50}$ map as measured after the intervention (2020) in dB(A).

on these topics, see e.g. [3]). Note, however, that the separation between MP1 and MP2 is only 50 m. Given this limited difference in propagation distance, such effects are expected to be rather limited which is consistent with the observed variation [3].

In addition, local disturbances near MP2 could lead to (momentary) incorrect highway noise transmission loss values. Similarly, periods with congestion will not lead to a correct assessment of the efficiency of the measures. The relative importance of the aforementioned effects will be rather limited given the full month of continuous sound recordings, and the fact that median values of the distributions of $TL_{1-2,2017}$ and $TL_{1-2,2020}$ were used.

To validate the mobile measurements, which were performed during daytime hours only, the fixed measurement stations were consequently analyzed for daytime hours during this validation exercise. The efficiency of the intervention ϵ was 4.2 dB(A) based on the fixed stations. With the mobile measurements, at the closest position to MP2 (using the 5-m spatial resolution), a level reduction of 5.4 dB(A) was found for $\Delta L_{A,50}$. Given the large number of mobile measurements near MP2, full convergence is reached (<0.1 dB(A), see Appendix A), both in 2017 and 2020. Note that an exact spatial match was not possible since MP2 was fenced to protect the microphone, while the average mobile microphone heights were somewhat lower. This means that the difference between the fixed and the mobile measurement falls within the accuracy limits of both types of instrumentation. This analysis provides a sufficiently convincing validation of the mobile procedure for assessing the spatially dependent mitigation efficiency.

3.2. Spatial analysis of the intervention efficiency

3.2.1. Overall exposure

In Figs. 7 and 8, the $L_{A,50}$ maps for 2017 and 2020 are shown. Before the intervention (Fig. 7), large exposures on the bridges (near 80 dB(A)) were measured, and levels on the cycling path exceed 70 dB(A) in most parts. In the first street behind the (interrupted) row of buildings, smaller levels are found, roughly 60 dB(A) directly behind the buildings. In zones with direct view towards the highway, in between the building blocks, slightly higher levels are measured. In the enclosed streets further away from the highway, levels drop considerably to a minimum of $L_{A,50}$ equal to 50 dB(A).

The two major roads in line with the bridges, bordering the triangular region that was assessed, give somewhat higher sound exposure levels, with strong local variations due to local events, e.g. by the many traffic lights at crossings leading to accelerating traffic. Given the too limited number of measurement there, levels are not converged and are only indicative (see Appendix A). After the intervention (Fig. 8), the part of the cycling path running below Bridge 2 has been assessed as well, and also the playground in between building block C and D (see Fig. 2).

3.2.2. Abatement efficiency along the cycling path

Fig. 9 depicts the difference ($\Delta L_{A,50}$) between the two maps shown in Figs. 7 and 8. Only the cycling path and the first street parallel to the highway are shown, where convergence within 0.5 dB(A) is reached at almost any point (see Appendix A). Note that level reductions are shown as integers in line with the measurement accuracy of the mobile equipment used. Along the cycling path, a strong variation in the abatement efficiency is observed, ranging from 5 dB(A) to 14 dB(A).

The minimum abatement of 5 dB(A) is observed at the crossing between the continuation line of the cutting through the berm and the cycling path, close to the fixed measurement station MP2 (see Fig. 9). At both sides of this specific zone, a higher noise reduction of 7 to 9 dB(A) is found. Further analysis shows that $\Delta(L_C - L_A)$ is only -1 dB at this spot, while it is -3 dB next to it (see Fig. 10). This shows that the relative increase in the low frequency content, as can be expected from an intervention like a raised berm, whose working principle relies largely on diffraction of sound, is not found here. Sound is thus able to propagate almost unhindered from a stretch of the highway to this point along the cutting, making this a dominant contribution. A similar conclusion can be made based on the analysis of ΔCOG (not shown), giving a shift in sound frequency of only 66 Hz, while around this spot this shift approaches 200 Hz.

The maximum abatement efficiency along the cycling path is 14 dB(A) (see Fig. 9). This is observed at the old branch of the cycling path near Bridge 2, located behind two successive berms after the intervention was put in place (see Fig. 4 a and Fig. 5, profile 2). Note that this rather large effect is measured under ideal conditions, namely very close behind the second berm, and at a low receiver height (ear height). This double diffraction leads to an $L_C - L_A$ equal to 11–12 dB during the 2020 campaign in this part

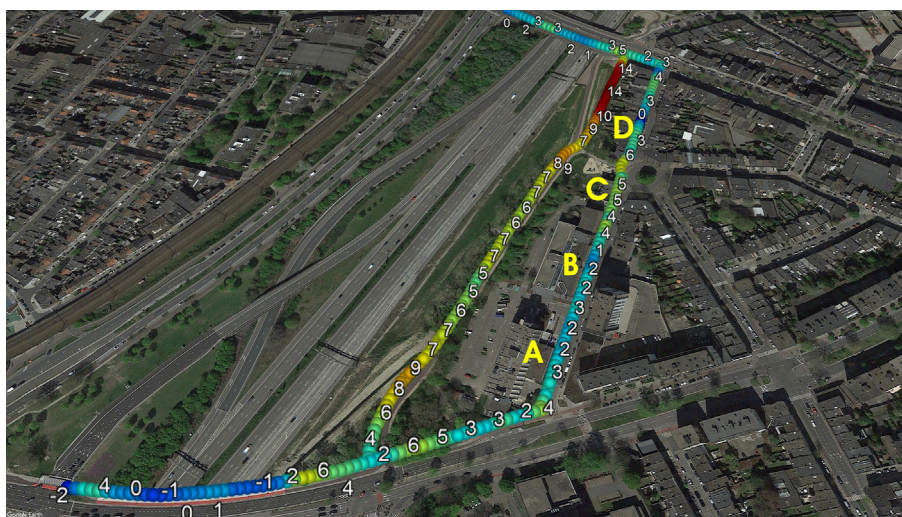


Fig. 9. $\Delta L_{A,50}$ map in dB(A).

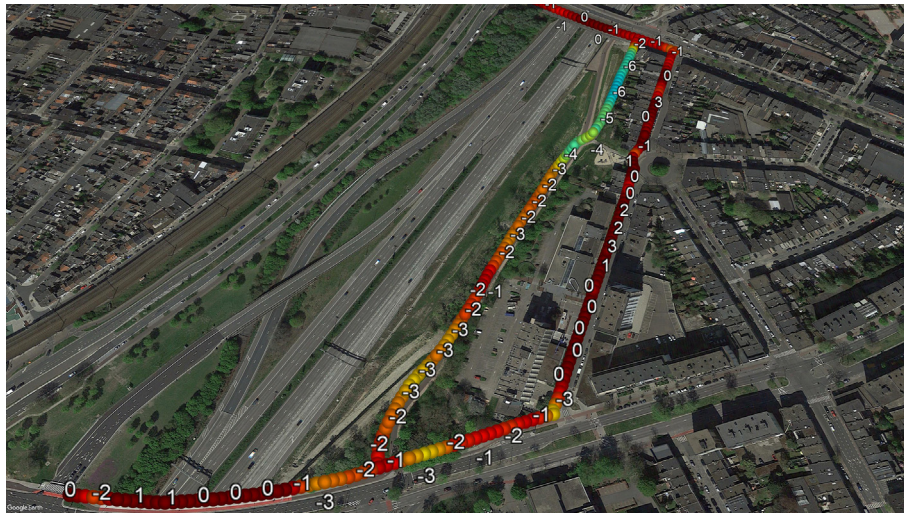


Fig. 10. $\Delta(L_C - L_A)$ map in dB.



Fig. 11. Detail of $L_C - L_A$ map (in dB) in the part running towards the underpass below Bridge 2, after the intervention.

(see Fig. 11); the $\Delta(L_C - L_A)$ equals -6 dB (see Fig. 10). Similarly, a large ΔCOG is observed here (not shown) equal to 448 Hz in the middle of this part. All these indicators show that sound arrives in this zone upon diffraction, favoring the low frequency part of the road traffic noise spectrum. This strong level reduction disappears quickly when approaching the local road in line with Bridge 2. There, the highway noise is not dominant anymore, and the impact of an intervention aiming at highway noise reduction is consequently limited.

At the new branch of the cycling path, a remarkable gradient in exposure level is measured when going from the part in between the two berms to the zone just in front of Bridge 2, bordered by the gabion walls (see Fig. 2 and Fig. 4 a,e). $L_{A,50}$ increases from 59 to 71 dB(A) over a few tens of meters (see Fig. 8), while $L_C - L_A$ drops from 12 to 6 dB (see Fig. 11). The gabion noise walls seem to perform poorly as a diffraction device, possibly due to insufficient acoustic insulation of the wall, giving rise to strong transmission through its structure. The COG behind the gabions was equal to 500 Hz, while in between the two berms it was only 375 Hz. For

comparison, on the bridges, with more or less direct line-of-sight propagation, values of about 700 Hz were found.

3.2.3. Abatement efficiency behind first row of buildings

In the street behind the first line of buildings, parallel to the cycling path and the highway, noise abatements by the interventions are generally limited. There are two distinct interruptions, between building blocks A and B (see Fig. 1), and between building blocks C and D (see Fig. 2). In the middle of blocks B and D (see Fig. 9), $\Delta L_{A,50}$ tends to zero, as the shielding provided by these buildings is dominant relative to the shielding provided by the raised berm; the highway noise intervention thus gives no additional benefit at these specific locations.

At the open spots between building A and B, and between C and D, there is direct sight towards the highway. In these zones, the abatement efficiencies are higher than at other locations in this street. In between buildings A and B, $L_{A,50}$ reduces with about 3 dB(A), while near the playground (between buildings C and D) reductions between 5 and 7 dB(A) are measured. Note that in

between the cycling path and the playground, a berm of limited height was present as well (see Fig. 2). These positive effects extend somewhat further along the street as well, due to the presence of more oblique sound paths being shielded by the highway intervention. Around the small building block C, a combination of the previous effects is observed. Near the ends of this street, levels are less reliable (see Appendix A) due to local events at the crossing roads, where more passages would be needed to allow a thorough comparison between the 2017 and 2020 situation.

4. Discussion and conclusion

In this work, a mobile sound measurement procedure has been presented, where by repeatedly walking a number of predefined paths, a detailed assessment of a highway noise abatement intervention is made. Although the mobile measurements are not standardized, a convincing validation of its ability to correctly measure the noise reducing efficiency is provided by comparing to a fixed continuously measuring type-1 microphone station. The deviation between these two approaches stays within the measurement accuracy of both types of equipment. Furthermore, such deviations are trifling, certainly with respect to the strong spatially dependent efficiency as observed in the current zone. The latter would have been missed by the standard use of a limited number of fixed measurement stations only.

Non-acoustical constraints in bringing noise abatement solutions to practice have a large impact on the final abatement efficiency. In the current situation, preparatory works for a second underpass below Bridge 1 needed a cutting in the berm. Its effect was demonstrated by the more limited noise reduction obtained on the cycling path in the continuation of this cutting. Secondly, due to weight constraints, in the zone in front of the underpass below Bridge 2, the berm was not prolonged. The noise reducing measure positioned there was a gabion noise wall. To further reduce the weight of the gabion, a high surface density core was not used. The mobile measurements clearly revealed this non-optimal solution, as shown by the strong spatial gradient in exposure levels when coming from the zone bordered by the berms to the gabions.

The difference between C-weighted and A-weighted total levels ($L_C - L_A$), a more detailed acoustic indicator, nicely points at locations where the enhancement of the diffracted field, which is a main effect of a raised berm, was not met. Similarly, the spectral center-of-gravity (COG) lead to similar conclusions. Note that additional analyses are not limited to the indicators used here. To open this possibility, a sufficient temporal sampling frequency and the ability to measure at sufficient spectral detail (like 1/3 octave bands) is needed at the mobile equipment.

In general, not only a careful acoustic design of a noise abatement tailored to the local situation is important, but also a strict execution. The mobile measurement procedure is an interesting learning tool for spatial planners to show the impact of such practical constructional limitations, and identifies zones where further reductions in environmental noise exposure are possible.

The main drawback of the current mobile measurement procedure is that it is labor intensive. Many passages are needed along predefined paths to end up with converged noise indicators. In the current work, a large number of passages were made in 2017, and a more limited number in 2020. Since the main interest was the highway noise exposure along the cycling path, a constant noise source during the day hours, this number seemed sufficient as shown by both the validation exercise and convergence reached

within 0.5 dB(A) there (see Appendix A). For a more accurate assessment at the non-highway noise dominated streets, more mobile measurements would be needed. Individual passages of cars along the walking operator, or platoons of cars when traffic lights turn green, lead to the local sudden increases, as visible in the $L_{A,50}$ maps (see Fig. 7 and Fig. 8) in the region behind the cycling path. At multiple spots, the convergence indicator exceeds 2 dB(A) as shown in Fig. A1. Opportunistic sampling could be an interesting approach to increase the number of measurements, e.g. by equipping city guards, postmen or bicycles from sharing systems with a microphone. Such approaches have been reported for applications of mobile air quality monitoring (see e.g. [10,21,22]).

Note that the noise abatement efficiency of the complex berm structures, as actually constructed, would be very hard to predict even with advanced noise mapping methodologies, making measurements at high spatial resolution useful anyhow. Even in the reference situation, with the gradually sloping talud and a ground impedance discontinuity, advanced numerical procedures were needed for an accurate estimation of the reference exposure levels [17].

CRediT authorship contribution statement

Timothy Van Renterghem: Conceptualization, Data curation, Formal analysis, Methodology, Validation, Visualization, Writing - original draft, Writing - review & editing. **Pieter Thomas:** Methodology, Writing - review & editing. **Luc Dekoninck:** Methodology, Writing - review & editing. **Dick Botteldooren:** Conceptualization, Methodology, Writing - review & editing.

Declaration of Competing Interest

The authors declare that they have no known competing financial interests or personal relationships that could have appeared to influence the work reported in this paper.

Acknowledgements

The authors are grateful to AG Vespa and the city of Antwerp for partly funding the data collection leading to this work. The authors appreciate the provision of drawings of the plans and cross-sections of the zone under study by Technum, forming the basis for Figs. 1, 2 and 5.

Appendix A: $L_{A,50}$ convergence map of the mobile measurements

As a convergence check, considering 80% of the data is compared to using all available data at each spatial aggregation point. A small level difference means that the measured levels are strongly converged. A large value, in contrast, indicates that more passages with the mobile microphones would be needed.

In Fig. A1, this convergence indicator for $L_{A,50}$, in both 2017 and 2020, are shown. The data indicates that along the cycling path, levels are strongly converged (<0.5 dB(A) at any point). In the street behind the first row of buildings, the convergence indicator is still small overall, but at a few spots near 1 dB(A). In the zone further away, which was not the focus of the current research and analysis, convergence is not reached; at many points, the convergence indicator exceeds 2 dB(A).

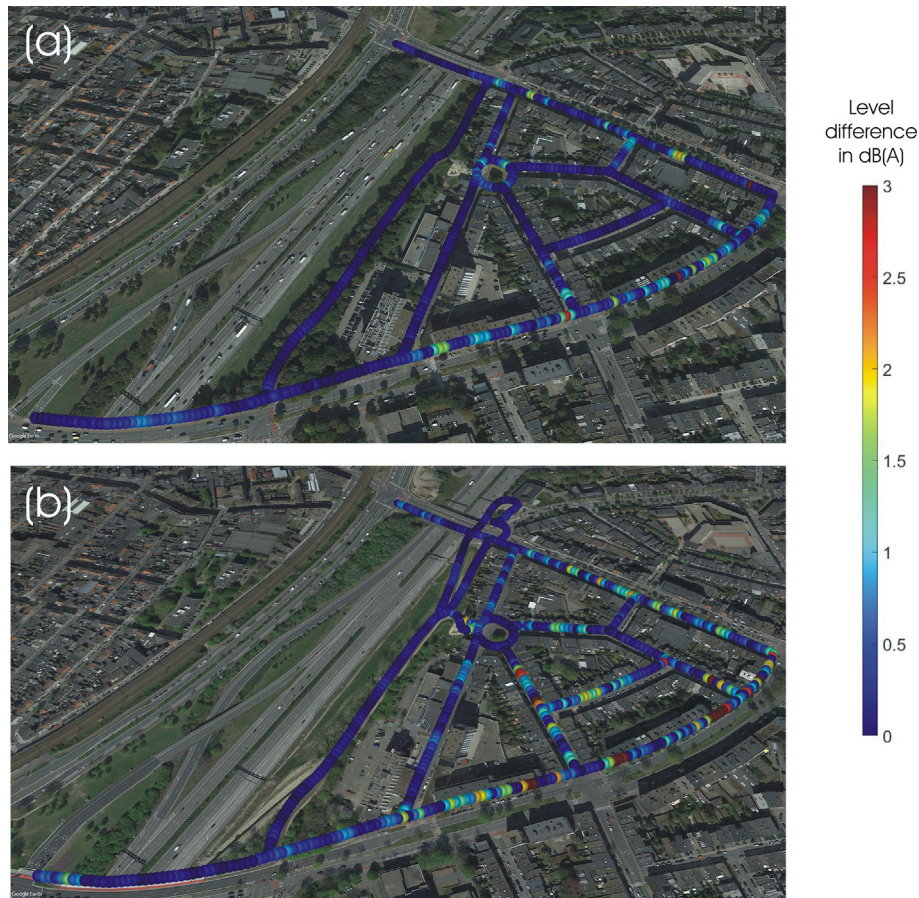


Fig. A1. Convergence indicator map for $L_{A,50}$ at each spatial aggregation point during the 2017 (a) and 2020 (b) mobile measurement campaigns. A level difference of 0 dB(A) means fully converged data.

References

- [1] Hänninen O, Knol A, Jantunen M, Lim T-A, Conrad A, Rappolder M, et al. Environmental burden of disease in Europe: Assessing nine risk factors in six countries. *Environ Health Perspect* 2014;122:439–46.
- [2] Kotzen B, English C. *Environmental Noise Barriers: A guide to their acoustic and visual design*. second ed. London and New York: Taylor and Francis, Spon Press; 2009.
- [3] Attenborough K, Van Renterghem T. *Predicting Outdoor Sound*. second edition. Boca Raton: Taylor and Francis, CRC Press; 2021.
- [4] Hadden W, Pierce A. Sound diffraction around screens and wedges for arbitrary point source locations. *J Acoust Soc Am* 1981;69:1266–76.
- [5] Jonasson H. Sound reduction by barriers on the ground. *J Sound Vib* 1972;22:113–26.
- [6] Embleton T. Tutorial on sound propagation outdoors. *J Acoust Soc Am* 1996;100:31–48.
- [7] Kanjo E. Noise SPY: A real-time mobile phone platform for urban noise monitoring and mapping. *Mobile Netw Appl* 2010;15:562–74.
- [8] D'Hondt E, Stevens M, Jacobs A. Participatory noise mapping works! An evaluation of participatory sensing as an alternative to standard techniques for environmental monitoring. *Pervasive Mob Comput* 2013;9:681–94.
- [9] Can A, Dekoninck L, Botteldooren D. Measurement network for urban noise assessment: Comparison of mobile measurements and spatial interpolation approaches. *Appl Acoust* 2014;83:32–9.
- [10] Dekoninck L, Botteldooren D, Int Panis L. Using city-wide mobile noise assessments to estimate bicycle trip annual exposure to Black Carbon. *Environ Int* 2015;83:192–201.
- [11] Quintero G, Aumond P, Can A, Balastegui A, Romeu J. Statistical requirements for noise mapping based on mobile measurements using bikes. *Appl Acoust* 2019;156:271–8.
- [12] Can A, Van Renterghem T, Rademaker M, Dauwe S, Thomas P, De Baets B, et al. Sampling approaches to predict urban street noise levels using fixed and temporary microphones. *J Environ Monit* 2011;13:2710–9.
- [13] Van Renterghem T, Thomas P, Dominguez F, Dauwe S, Touhafi A, Dhoedt B, et al. On the ability of consumer electronics microphones for environmental noise monitoring. *J Environ Monit* 2011;13:544–52.
- [14] Nast D, Speer W, Le Prell C. Sound level measurements using smartphone "apps": Useful or inaccurate? *Noise Health* 2014;16:251–6.
- [15] Kardous C, Shaw P. Evaluation of smartphone sound measurement applications. *J Acoust Soc Am* 2014;135:EL186–92.
- [16] Murphy E, King E. Testing the accuracy of smartphones and sound level meter applications for measuring environmental noise. *Appl Acoust* 2016;106:16–22.
- [17] Van Renterghem T, Botteldooren D. Landscaping for road traffic noise abatement: model validation. *Environ Modell Software* 2018;109:17–31.
- [18] Koussa F, Defrance J, Jean P, Blanc-Benon P. Acoustic performance of gabions noise barriers: numerical and experimental approaches. *Appl Acoust* 2013;74:189–97.
- [19] Van Renterghem T, Van Ginderachter I, Thomas P. Porous stones increase the noise shielding of a gabion. *Appl Acoust* 2019;145:82–8.
- [20] IEC 61672-1:2013, *Electroacoustics - Sound level meters - Part 1: Specifications*.
- [21] Van den Bossche J, Theunis J, Elen B, Peters J, Botteldooren D, De Baets B. Opportunistic mobile air pollution monitoring: A case study with city wardens in Antwerp. *Atmos Environ* 2016;141:408–21.
- [22] Liu X, Xiang C, Li B, Jiang A. Collaborative bicycle sensing for air pollution on roadway. 2015 IEEE 12th International Conference on Ubiquitous Intelligence and Computing - Autonomic and Trusted Computing - Scalable Computing and Communications; 2016.